Acta Pharmaceutica Sinica B 2023;13(1):174–191

Chinese Pharmaceutical Association
Institute of Materia Medica, Chinese Academy of Medical Sciences

Acta Pharmaceutica Sinica B

www.elsevier.com/locate/apsb
www.sciencedirect.com

ORIGINAL ARTICLE

Vitisin B inhibits influenza A virus replication by multi-targeting neuraminidase and virus-induced oxidative stress

Eun-Bin Kwon[a,†], Wei Li[a,†], Young Soo Kim[a], Buyun Kim[a], Hwan-Suck Chung[a], Younghoon Go[a], Hyun-Jeong Ko[d], Jae-Hyoung Song[d], Young Ho Kim[b,*], Chun Whan Choi[c,*], Jang-Gi Choi[a,*]

[a]*Korean Medicine (KM) Application Center, Korea Institute of Oriental Medicine, Daegu 41062, Republic of Korea*
[b]*College of Pharmacy, Chungnam National University, Daejeon 34134, Republic of Korea*
[c]*Natural Product Research Team, Biocenter, Gyeonggido Business and Science Accelerator, Gyeonggi-Do 16229, Republic of Korea*
[d]*Laboratory of Microbiology and Immunology, College of Pharmacy, Kangwon National University, Chuncheon 24341, Republic of Korea*

Received 13 January 2022; received in revised form 25 March 2022; accepted 16 June 2022

KEY WORDS

Influenza;
Vitisin B;
Vitis vinifera L.;
Neuraminidase;
Reactive oxygen species;
NF-κB;
Multi-targeting;
Nrf2;
G6PD

Abstract The development of drug-resistant influenza and new pathogenic virus strains underscores the need for antiviral therapeutics. Currently, neuraminidase (NA) inhibitors are commonly used antiviral drugs approved by the US Food and Drug Administration (FDA) for the prevention and treatment of influenza. Here, we show that vitisin B (VB) inhibits NA activity and suppresses H1N1 viral replication in MDCK and A549 cells. Reactive oxygen species (ROS), which frequently occur during viral infection, increase virus replication by activating the NF-κB signaling pathway, downmodulating glucose-6-phosphate dehydrogenase (G6PD) expression, and decreasing the expression of nuclear factor erythroid 2-related factor 2 (Nrf2) antioxidant response activity. VB decreased virus-induced ROS generation by increasing G6PD expression and Nrf2 activity, and inhibiting NF-κB translocation to the nucleus through IKK dephosphorylation. In addition, VB reduced body weight loss, increased survival, decreased viral replication and the inflammatory response in the lungs of influenza A virus (IAV)-infected mice. Taken together, our results indicate that VB is a promising therapeutic candidate against IAV infection,

*Corresponding authors. Tel./Fax.: +82 42 8215933/+82 42 8236566, +82 31 8886131/+82 31 8886139, +82 53 9403866/+82 53 9403899
E-mail addresses: yhk@cnu.ac.kr (Young Ho Kim), cwchoi78@gmail.com (Chun Whan Choi), Jang-gichoi@kiom.re.kr (Jang-Gi Choi).
[†]These authors made equal contributions to this work.
Peer review under the responsibility of Chinese Pharmaceutical Association and Institute of Materia Medica, Chinese Academy of Medical Sciences.

https://doi.org/10.1016/j.apsb.2022.07.001

complements existing drug limitations targeting viral NA. It modulated the intracellular ROS by G6PD, Nrf2 antioxidant response pathway, and NF-κB signaling pathway. These results demonstrate the feasibility of a multi-targeting drug strategy, providing new approaches for drug discovery against IAV infection.

1. Introduction

Influenza A virus (IAV) is a major respiratory pathogen according to the World Health Organization that readily mutates or rearranges into new strains. It causes high morbidity, mortality, and significant economic loss worldwide each year[1]. Influenza viruses are RNA viruses consisting of eight segments, including neuraminidase (NA) and hemagglutination (HA), which may yield new strains through mutation and gene rearrangement, and sometimes result in deadly strains[2,3].

Vaccines and antiviral agents are essential for mitigating the deleterious effects of the influenza virus. Antiviral drugs may be broadly classified into the amantadine class, polymerase inhibitors, and neuraminidase (NA) inhibitors (NAIs)[4,5]. Most US Food and Drug Administration (FDA)-approved drugs belong to NAIs, such as oseltamivir phosphate, zanamivir, and peramivir[6,7]. NAI is a class of drugs that block the viral NA protein and inhibit the release of the virus from the host cell, thereby preventing the subsequent infection of a new host cell[8]. Thus, NA has emerged as an attractive antiviral treatment target.

The development of drug resistance remains a concern for existing NAIs. The H274Y mutation is primarily found in oseltamivir-resistant clinical strains, such as seasonal A(H1N1), A(H1N1)pdm09, and the highly pathogenic A(H5N1) strains, and exhibits decreased NA enzymatic activity and oseltamivir resistance[9−11]. For the IAV strain, E119G is the most commonly associated with zanamivir resistance, although E119A and E119D have been reported to mediate resistance to other NAIs. For influenza B virus, E119G and E119D/A/V/G variants exhibit reduced susceptibility to zanamivir and peramivir, respectively. In addition, the R152K and R292K variants show reduced susceptibility to both[12−15]. Peramivir resistance is mainly conferred by an H274Y substitution in seasonal A(H1N1), A(H3N2), and A(H1N1)pdm09 viruses. Therefore, the development of new NAIs is warranted[12,16−19].

Redox homeostasis regulates the production of reactive oxygen species (ROS) through enzymatic antioxidant systems including superoxide dismutase (SOD), catalase (CAT), glutathione peroxidase (GPx), and glutaredoxin (GR)[20,21]. Increased expression of viral M2 protein during viral infection activates protein kinase C and increases ROS production[22,23]. In addition, IAV causes an imbalance in oxidative stress characterized by glutathione (GSH) depletion and upregulation of nicotinamide adenine dinucleotide phosphate (NADPH) oxidase (NOX)[24−26]. Moreover, proapoptotic influenza A virus protein (PB1-F2) suppresses ROS scavenging activity by decreasing SOD1 expression. Therefore, ROS are produced during IAV infection, which results in the activation of virus replication and promotes apoptosis, lung injury, and abnormal inflammation[21,27,28]. Excessive ROS production resulting from viral infection activates nuclear factor (NF)-κB signaling, which regulates the expression of viral and host genes involving in viral replication and the inflammatory response[29,30]. Nuclear factor kappa B (NF-κB) upregulates inflammatory cytokine levels, including interleukin (IL)-1β, IL-6, interferon (IFN), and tumor necrosis factor (TNF)-α, and triggers a cytokine storm[31−34].

The nuclear factor erythroid 2-related factor 2 (Nrf2) pathway is the principal protective oxidative stressor in host cells. Accumulation of oxidative stress led to Nrf2 translocating to the nucleus and then binding to antioxidant response elements. Activation of Nrf2 signaling increased the expression of genes associated with antioxidant enzymes, such as CAT, SOD, and GSH syntheses, which are related to glucose-6-phosphate dehydrogenase (G6PD). In contrast, previous report has shown that influenza A virus (H5N1 and H7N9) reduced phosphorylated Nrf2 within the nucleus, leading to enhanced viral replication and ROS induction[35,36]. Antioxidant therapy reduces viral load and prevents lung damage resulting from viral-induced ROS overproduction[37,38]. Therefore, regulating ROS plays a modulatory role in antiviral therapy. Developing effective therapeutic agents with fewer side effects may be possible by establishing synergistic effects. Thus, multi-targeting, rather than targeting a single protein or process to regulate viral proteins or oxidative stress, may be achieved.

Natural products have been shown to contribute to the drug development process for various diseases and the study has continued in the field of antiviral therapeutics[34]. Strong antiviral activity of traditional natural products has been demonstrated for preventing and treating viral infections, including severe acute respiratory syndrome coronavirus 2 (SARS-CoV-2) and influenza[39−43]. Recently, we demonstrated that natural products, including Geranii Herba, *Ohwia caudata*, *Rhus verniciflua*, and *Aloe vera*, exhibit antiviral activity against the influenza virus[44−47]. Therefore, these natural sources may contribute to the development of novel, effective antiviral agents.

Vitisin vinifera L. is used to treat various diseases including diarrhea, hemorrhage, varicose veins, hemorrhoids, inflammatory disorder, pain, and hepatitis. It also exhibits anti-inflammatory properties[48]. Although several studies have demonstrated the antiviral activity of *V. vinifera* against herpes simplex virus type 1 (HSV-1), severe acute respiratory syndrome coronavirus 2 (SARS-CoV-2), and hepatitis C virus, no reports exist regarding the antiviral effects of *V. vinifera* stem bark extracts for treating influenza viral infections[49,50].

Therefore, we evaluated the anti-influenza activity of 12 compounds isolated from *V. vinifera* stem bark using an NA inhibition assay. In addition, this is the first study to identify vitisin B (VB) as the active compound of *V. vinifera* stem bark that inhibits NA. The results suggest that VB is an emerging candidate for the development of novel antiviral agents that prevent and treat influenza virus infections.

2. Materials and methods

2.1. Reagents

RPMI 1640 and Dulbecco's modified Eagle's media (DMEM) were purchased from Hyclone (Pittsburgh, PA, USA) and an enhanced chemiluminescence (ECL) reagent was purchased from ThermoFisher Scientific (Waltham, MA, USA). MitoSOX and DCF-DA were purchased from Invitrogen (Carlsbad, CA, USA). The PRO-PREP protein extraction solution was purchased from Intron Biotechnology (Seoul, Republic of Korea). Antibodies against M1, M2, PA, and NS1 were obtained from GeneTex, Inc. (Irvine, CA, USA). The 3-(4,5-dimethylthiazol-2-yl)-2,5-diphenyltetrazolium bromide (MTT) was purchased from Sigma−Aldrich (St. Louis, MO, USA).

2.2. Cells and viruses

The A549 human lung epithelial cell line and Madin−Darby canine kidney (MDCK) cells were obtained from the American Type Culture Collection (Manassas, Virginia, USA). The A549 cells were grown in RPMI 1640 containing 10% fetal bovine serum (FBS; Gibco, Grand Island, NY, USA) and 1% antibiotic−antimycotic at 37 °C in a 5% CO_2 atmosphere, whereas MDCK cells were cultured in DMEM containing 10% FBS and 1% antibiotic−antimycotic at 37 °C in a 5% CO_2 atmosphere. The GFP-encoding influenza A strains (A/PR8/34-GFP) and Puerto Rico/8/34 viruses have been used in previous studies[39]. Oseltamivir-resistant Puerto Rico/8/34(A/PR8/34) viruses were obtained from Prof Hyun-Jeong Ko (Kangwon National University, Chuncheon, Republic of Korea)[51]. KBPV-VR-32 (H3N2; A/Korea/33/2005) and influenza B (B/Korea/72/2006) viruses were purchased from the Korea Bank for Pathogenic Viruses.

2.3. Plant materials

The stem bark of *V. vinifera* was harvested in October 2008 from a vineyard in Yuseong, Korea. A voucher specimen (KR0331) was deposited at the herbarium of the Korea Research Institute of Chemical Technology (Seoul, Republic of Korea).

2.4. Extraction and isolation

The stem bark of *V. vinifera* (10 kg) was extracted twice with ethanol by maceration for seven days. The resulting filtrate was combined and evaporated to dryness to yield a 708.8 g extract. The ethanol extract was suspended in water and sequentially partitioned with an equal volume of CH_2Cl_2, EtOAc, and *n*-BuOH. The EtOAc-soluble fraction (463.8 g) was separated by silica gel (5.0 kg) column chromatography (MeOH/CH_2Cl_2 1%−50%) to yield six fractions. Lupenone (15 mg), lupeol (25 mg), and botulin (20 mg) were isolated from fraction (Fr. 1). Vitisin A (90 mg), *cis*-vitisin A (8.1 g), VB (9.1 g), malibatol A (48 mg), and *ε*-viniferin (230 mg) were isolated from Fr. 2. Ampelopsin A (15 mg), (+)-viniferether B (13 mg), caraphenol B (15 mg), and resveratrol (9 mg) were isolated from Fr. 3 (Supporting Information Table S1 and Scheme S1).

2.5. NA assay

The NA-Fluor Influenza Neuraminidase Assay Kit (Applied Biosystems, Foster City, CA, USA) was used to measure the NA activity according to the manufacturer's instructions. Briefly, VB was combined with an assay buffer in a 96-well plate at 0−100 μmol/L for H1N1, H3N2, and influenza B viruses. Next, H1N1, H3N2, or influenza B were added to the VB-containing wells and incubated at 37 °C. Oseltamivir was used as a positive control in the assay. After 30 min, NA-Fluor substrate was added to each well and incubated for extra 2 h followed by measurement (excitation: 365 nm; emission: 415−445 nm) with a fluorescence spectrophotometer (Promega, Madison, WI, USA).

For the NA-XTD influenza neuraminidase assay, VB or oseltamivir carboxylate were added to the assay buffer in 96-well plates at 0−100 μmol/L for oseltamivir-resistant A/PR8/34. Subsequently, oseltamivir-resistant A/PR8/34 in assay buffer was added to VB or oseltamivir carboxylate-containing wells and incubated at 37 °C. Oseltamivir carboxylate was considered as the positive control in the assay. After 20 min, NA-XTD substrate was added to each well and incubated for an additional 30 min. Next, NA-XTD accelerator was added to each well, followed by recording the luminescence using a luminescence plate reader (Promega, Madison, WI, USA).

2.6. In vitro assessment of antiviral effect

The antiviral effect of VB was determined based on the inhibition of viral cytopathies, and the degree of cell viability was measured using MTT assay. MDCK cells were infected with H1N1, H3N2, and IBV, and A549 cells were infected with oseltamivir-resistant A/PR8/34 virus at a VB concentration of 0.1, 1, 10, and 20 μmol/L. After 24 h, 0.5 μg/mL MTT solution was added and formation of purple formazan was dissolved using DMSO. The absorbance at 540 nm was recorded using Microplate Reader (BioTek, USA).

2.7. MTS assay

According to the manufacturer's instructions, cell viability was determined using the CellTiter 96 AQueous One Solution Cell Proliferation Assay (Promega, Madison, WI, USA). MDCK (1×10^5 cells/well) and A549 (1×10^5 cells/mL) cells were seeded into 96-well plates, and VB was added to the wells at 0−200 μmol/L. After 48 h, MTS solution was added, and the cells were incubated for an additional 2 h. The absorbance at 490 nm was recorded using a GloMax Explorer Multimode Microplate Reader (Promega, Madison, WI, USA). The values from the MTS assay are presented as the mean ± standard error of mean (SEM) of four independent experiments.

2.8. Detection of GFP expression

MDCK and A549 cells were seeded into 24-well plates (1×10^5 cells/mL) for 24 h. For the co-treatment assay, VB PR8/34-GFP (multiplicity of infection [MOI] = 10) was added to VB at different concentrations (1, 10, and 50 μmol/L) and incubated at 4 °C for 2 h. Cells were infected with a mixture of VB and viruses at 37 °C for 2 h. Then, the viruses were removed, the cells were washed with phosphate-buffered saline (PBS), and the medium

was replaced with a complete media. After 24 h, viral GFP expression was observed under a fluorescence microscope, and quantitative analysis was done by flow cytometry (CytoFLEX; Beckman Coulter Inc., Pasadena, CA, USA).

2.9. Real-time quantitative-polymerase chain reaction (RT-PCR)

According to the manufacturer's instructions, total RNA was extracted from cell lysates using Trizol kit. Also, using the same technique, RT-PCR was performed using AccuPower 2 × Greenstar qPCR Master Mix (Bioneer, Daejeon, Republic of Korea) and a CFX96 Touch Real-Time PCR System (Bio-Rad, Hercules, CA, USA). The sense and antisense primer sequences are listed in Supporting Information Table S2.

2.10. Western blotting

Cells were lysed using the PRO-PREP protein extract solution on ice for 30 min. Then, the supernatant was collected after centrifugation at 13,200 × *g* for 30 min at 4 °C. The Bradford method was used to determine the protein concentration. Protein samples were separated by sodium dodecyl sulfate-polyacrylamide gel electrophoresis (SDS-PAGE, 8%−15% gel) and transferred to polyvinylidene fluoride (PVDF) membranes. After blocking with 0.5 × Ez-Block Chemi (Amherst, MA, USA), the blots were incubated with antibodies and detected using the ChemiDoc imaging system (UVITEC, Cleaver Scientific Ltd., UK) with an enhanced chemiluminescence reagent (ThermoScientific, Rockford, IL, USA).

2.11. Hemagglutination (HA) assay

According to studies, chicken red blood cells were diluted to 0.5% using cold PBS. Then, a mixture containing 0.5% chicken red blood cells and the diluted sample was incubated on round bottom plates at room temperature, imaged, and counted.

2.12. Immunofluorescence (IF)

After coverslip coating with poly-D-lysine (Gibco, USA) for 15 min, A549 cells were seeded at 1×10^5 cells/mL for 24 h. The cells were treated with a virus mixture and incubated at 37 °C for 24 h. They were then fixed with 4% paraformaldehyde in PBS for 10 min at room temperature and washed three times with PBS. The cells were incubated with a blocking solution (5% BSA in PBS) for 30 min followed by NF-κB and Nrf2 antibodies overnight at 4 °C for 24 h. After the reaction, the cells were washed with PBS and incubated with secondary antibody for 30 min on a rocker. Finally, they were washed with PBS and stained with Hoechst 33342 for 15 min. The coverslips were mounted on slides using a mounting medium and were visualized using a fluorescence microscope (Lionheart FX automated microscope, BioTek, USA).

2.13. Isolation of nuclear protein

Cells were lyzed in a lysis buffer with pH value of 7.8 containing Tris (10 mmol/L), KCl (10 mmol/L), EDTA (0.1 mmol/L), $MgCl_2$ (1.5 mmol/L), Nonidet P-40 (0.2%), dithiothreitol (0.5 mmol/L), Na_3VO_4 (1 mmol/L), and phenylmethylsulfonyl fluoride (PMSF, 0.4 mmol/L). The nuclei were pelleted at 1000 × *g* for 5 min at 4 °C and resuspended in an extraction buffer with pH value of 7.8 containing Tris (20 mmol/L), NaCl (420 mmol/L), EDTA (0.1 mmol/L), $MgCl_2$ (1.5 mmol/L), glycerol (20%), dithiothreitol (0.5 mmol/L), Na_3VO_4 (1 mmol/L), and PMSF (0.4 mmol/L). The nuclear extracts were then centrifuged at 10,000 × *g* for 5 min divided into aliquots in chilled tubes, frozen quickly in liquid nitrogen, and stored at −70 °C. Protein concentration was determined by a BCA kit.

2.14. Antioxidant related enzyme activity

A549 cells were infected with IAV in 20 μmol/L VB for 24 h. According to the manufacturer's instructions, GSH/GSSG ratio in cell lysate was measured using an Ez-glutathion kit (Dogen), and activities of CAT and SOD in cell lysate were measured using CAT assay kit and SOD assay kit, respectively (Cayman).

2.15. ROS

A549 cells were infected with IAV and co-treated with various concentrations of VB (1, 10, or 20 μmol/L) for 24 h. The cells were incubated with 1 μmol/L MitoSOX at 37 °C for 30 min and washed with PBS for mitochondrial superoxide activity. The cells were harvested by trypsinization for ROS quantitation, resuspended in 0.5-mL PBS, incubated with 5 μmol/L H2DCF-DA or 2 μmol/L dihydroethidium (HE), and analyzed by flow cytometry (cytoFLEX, Beckman Coulter Inc., Brea, CA, USA).

2.16. The electrophoretic mobility shift assay (EMSA)

Nuclear extracts were prepared as mentioned above. EMSA for DNA-binding activity of NF-κB was conducted with a nonradioactive EMSA kit (Roche, Mannheim, Germany). The binding activity of NF-κB-p65 in the influenza-infected cells was confirmed by EMSA with a DIG-labeled oligonucleotide (NF-κB: 5′-AGT TGA GGG GAC TTT CCC AGG C-3′). The nuclear extract and the labeled oligonucleotide (Invitrogen) were incubated in a binding buffer at room temperature for 1 h, and subsequently, the mixture was subjected to electrophoresis on a nondenatured polyacrylamide gel (6%), followed by an electrotransfer to a positively charged nylon membrane. The membrane was subsequently treated with anti-digoxigenin-Ap Fab fragments (Roche). The chemiluminescent substrate CSPD (Roche) was added, and the resulting chemiluminescence was detected by autoradiography. The specificity of the NF-κB-binding complex was tested by adding excess unlabeled oligonucleotide.

2.17. In vivo experiment

This study was performed following the guidelines of and approved by the Institutional Animal Care and Use Committee of the Laboratory Animal Center of Daegu-Gyeongbuk Medical Innovation Foundation (DGMIF, DGMIF- 21010605-00). Female BALB/c mice (5 weeks old) from Orient Bio Inc. (Seongnam, Republic of Korea) were acclimated for at least one week under standard housing conditions at DGMIF. A standard rodent chow diet and water were administered *ad libitum*. The mice were separated into three experimental sets containing three groups of 10 mice per set (PBS, VB [20 mg/kg] with virus infection, oseltamivir [OP, 20 mg/kg], and PBS with virus infection). Mice were infected intranasally with a 50% murine lethal dose (LD_{50}) of A/PR/8/34 five times in 20 μL of PBS and orally administered with 20 mg/kg VB, OP, and PBS in a total volume of 200 μL, once daily for 13 days after virus infection. The survival rate was determined when the mouse died and the bodyweight decreased

by 20%. Body weights and survival were monitored for 13 days post-infection (dpi) at fixed time points. At 8 dpi, three mice from each group were randomly sacrificed to measure lung histopathology, and the remaining were used to examine survival. Lung tissues were immediately fixed in paraffin-embedded neutral buffer containing 10% formalin, sectioned to 4−6 μm thickness using a microtome, mounted onto slides, stained with eosin, and examined under an optical microscope.

2.18. *In silico docking simulation and pharmacophore analysis*

The H1N1 NA crystal structure (PDB code: 3TI6) was used as a receptor for docking simulations. VB (ChemSpider ID: 17290428) and the positive control, oseltamivir carboxylate (PubChem CID: 449381), were prepared by adding hydrogen to the molecules as ligands. VB and oseltamivir carboxylate were docked onto a predefined area with a 25 × 25 × 25 dimension using AutoDock Vina integrated with UCSF Chimera 1.15. The binding affinity of VB and oseltamivir carboxylate to H1N1 NA is presented as the lowest energy score of the docking simulation. In addition, the molecular interactions between H1N1 NA and VB/oseltamivir carboxylate were analyzed using the BIOVIA Discovery Studio Visualizer.

2.19. *Cytokines*

IL-6 and TNF-α (mouse) levels in mouse blood serum were measured using ELISA antibody kits (eBioscience), according to the manufacturer's instructions.

2.20. *Statistical analysis*

Data are expressed as mean ± SEM. Statistically significant differences in the mean values between the treatment and control

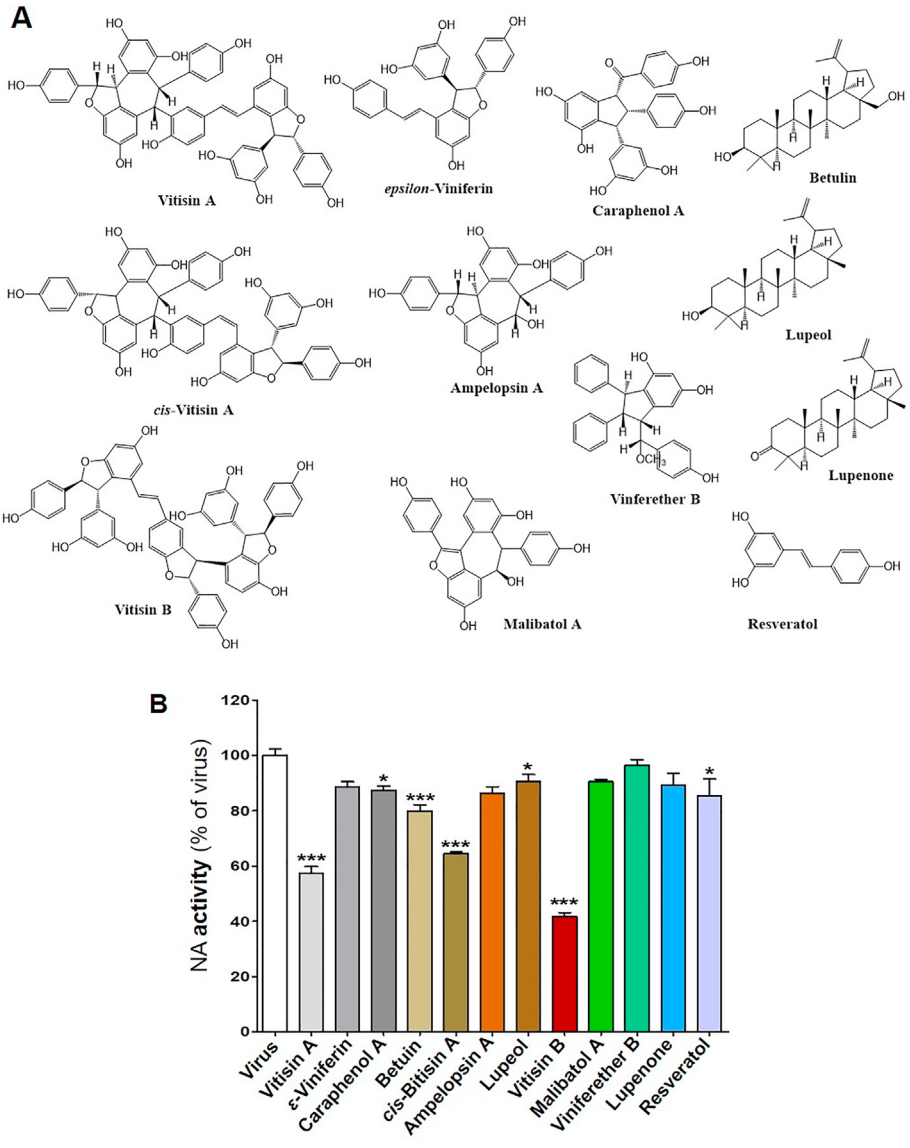

Figure 1 Effects of the major compounds isolated from *Vitis vinifera* L. on neuraminidase (NA) activity. (A) Twelve major compounds isolated from *Vitis vinifera*. (B) Measurement of the antiviral effect of the major components at 10 μmol/L using an NA inhibition assay against influenza A virus (A/PR/8/34). Bar graph (mean ± SEM) statistics were determined by the results of experiments ($n = 6$) using a one-way ANOVA with Tukey's *post hoc* test, $^{***}P < 0.001$; $^{**}P < 0.05$, compared with the virus-infected group (virus).

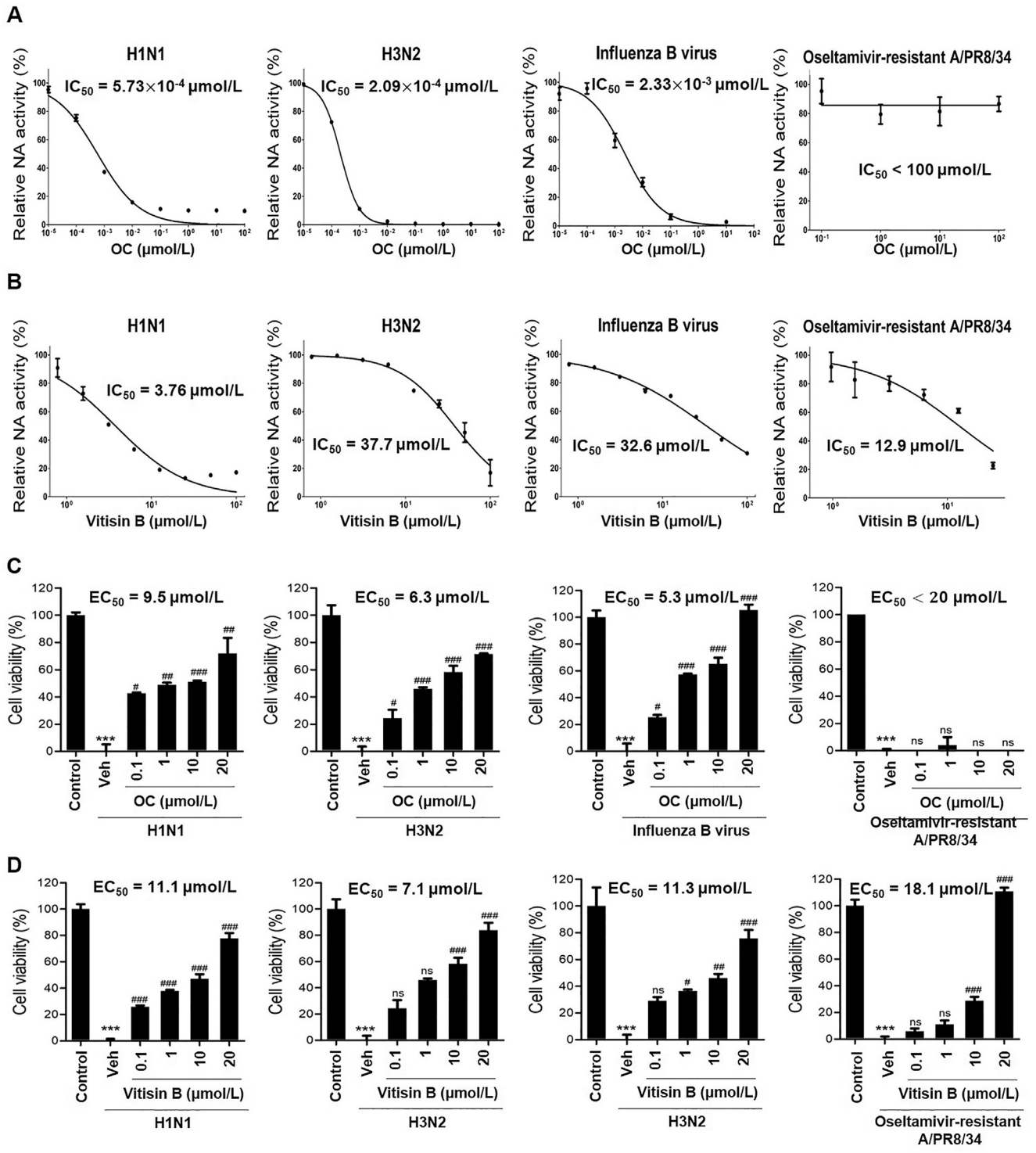

Figure 2 Determination of neuraminidase (NA) inhibition activity of vitisin B. Influenza viruses, including H1N1(A/PR/8/34), H3N2, and influenza type B, were treated with the indicated concentrations of (A) oseltamivir carboxylate (OC) and (B) vitisin B. NA inhibition was measured using NA activity kit. Antiviral activity of vitisin B and OC against various viruses, including H1N1, H3N2, and influenza B virus in MDCK cells and oseltamivir-resistant A/PR8/34 viruses in A549 cells were conducted. The cells were infected with viruses at various (C) vitisin B and (D) OC concentrations. Cell viability was analyzed by MTT assay and measured based on the OD of samples at 540 nm. Veh: Vehicle as virus infection group. Bar graph (mean ± SEM) statistical analysis was performed using results of experiments ($n = 6$) using a one-way ANOVA with Tukey's *post hoc* test, $^{***}P < 0.001$ compared with the untreated group (Control). $^{\#\#\#}P < 0.001$; $^{\#\#}P < 0.01$; $^{\#}P < 0.05$ compared with the virus-infected group (Veh). ns, not significance.

groups were determined using a Chi-squared test and Bonferroni's correction. ANOVA was performed using Bonferroni's *post hoc* test to analyze three or more groups. Survival analysis was performed using the Kaplan−Meier method, and the statistical significance of differences was determined using the log-rank test. Analyses were performed using GraphPad PRISM software v.5.02 (GraphPad, La Jolla, CA, USA). Statistical significance was set at $P < 0.05$.

3. Results

3.1. Inhibitory effect of VB isolated from Vitisin vinifera L. on NA activity

NAIs have an important role in preventing the spread of influenza infection by inhibiting NA activity, a surface glycoprotein of influenza virus. We evaluated the effect of 12 compounds isolated from *Vitisin vinifera* L., including resveratrol and resveratrol condensation products, on IAV NA activity (Fig. 1A). The results indicate that vitisin A, *cis*-vitisin A, and vitisin B inhibited NA activity by 43%, 35%, and 58%, respectively (Fig. 1B). NA inhibition experiments were conducted for the H1N1 and H3N2 types of influenza A and B viruses using vitisin B. The results indicate that vitisin B treatment resulted in a 50% NA inhibitory effect on H3N2 and influenza B viruses at 37.7 and 32.6 μmol/L, respectively (Fig. 2A), whereas it showed a 50% NA inhibitory effect in H1N1 at 3.76 μmol/L (Fig. 2B). Furthermore, we investigated whether VB exhibited NA activity against oseltamivir (OC)-resistant A/PR8/34 viruses. As shown in Fig. 2A and B, OC had no effect on OC-resistant viruses; however, VB treatment resulted in a 50% NA inhibition at 12.9 μmol/L. Collectively, these results indicate that vitisin B significantly inhibited NA activity of the H1N1 influenza virus and vitisin B exhibited antiviral effects by inhibiting the release of virus following NA inhibition.

3.2. In vitro antiviral effects of VB on influenza and oseltamivir-resistant A/PR8/34 viruses

Due to examining the antiviral effect of VB on influenza viruses, including H1N1, H3N2, IBV, and OC-resistant viruses, the data confirmed that VB showed EC_{50} values of 11.1 (H1N1), 7.1 (H3N2), and 11.7 μmol/L (IBV). In addition, OC showed EC_{50} values of 9.5 (H1N1), 6.3 (H3N2), and 5.3 μmol/L (IBV) in MDCK cells. We analyzed the antiviral effect of VB on OC-resistant viruses in A549 cells. VB showed EC_{50} values of 18.1 μmol/L (OC-resistant A/PR8/34) but OC was not effective against OC-resistant A/PR8/34 viruses (Supporting Information Fig. S1). These results suggest that VB is an effective antiviral agent against influenza A and B viruses and those resistant to the NA inhibitor OC (Fig. 2C and D).

3.3. Antiviral effects of VB on IAV-infected MDCK and A549 cells

Based on the above results, we determined whether VB inhibits the viral replication of influenza A of H1N1 virus-infected MDCK and A549 cells. An influenza virus-encoding green-fluorescent protein (GFP) was used. Prior to the experiment, an MTS assay was carried out with various concentrations of VB (0−200 μmol/L) to determine whether it exhibits cytotoxicity in MDCK and A549 cells (Fig. 3A and B). VB was cytotoxic at 100 μmol/L in A549 cells and at 200 μmol/L in MDCK cells. Therefore, we determined whether VB inhibited viral infection by treatment with a range of concentrations below 50 μmol/L, which did not show cytotoxicity in the MTS assay.

VB inhibits viral GFP expression in MDCK and A549 cells (Fig. 4A and B). GFP expression was quantified by flow cytometry. VB inhibited viral GFP by 93% and 91% in MDCK and A549 cells, respectively, at 50 μmol/L (Fig. 4C and D). VB also inhibited virus infection in a concentration-dependent manner through HA (Fig. 4E). VB decreased the expression of viral genes including matrix protein (M1), non-structural protein 1 (NS1), polymerase acidic protein (PA), and PB1, in MDCK cells (Fig. 4F). Immunofluorescent images further indicated that VB decreased the NA viral protein at 50 μmol/L compared with the virus control (Fig. 4G). The expression of viral proteins in A549 and MDCK cells treated with influenza and VB were confirmed by Western blot analysis. As shown in Fig. 4H−K, VB decreased viral protein expression in a dose-dependent manner compared with that of the influenza virus. Taken together, these results indicate that VB suppressed viral infection by reducing the expression of viral genes, including NA, PA, and PB1, in MDCK and A549 cells.

3.4. Protein−ligand docking simulation and pharmacophore analysis of VB

We evaluated the binding affinity of VB to H1N1 NA (PDB code: 3TI6), which is responsible for releasing progeny virions from

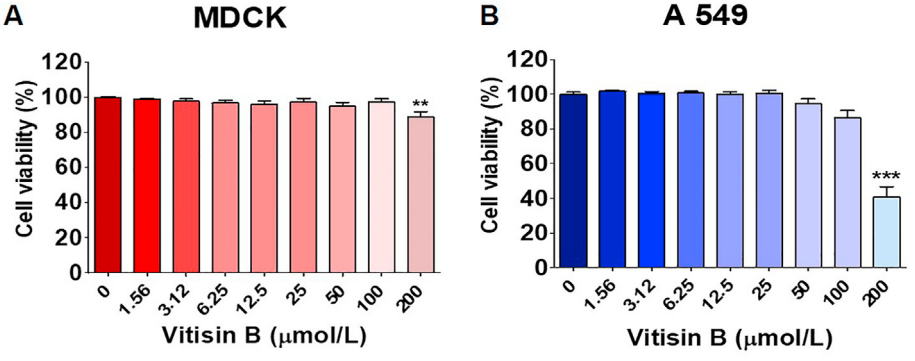

Figure 3 Effects of vitisin B on Madin−Darby canine kidney (MDCK) and A549 cell viability. The cells were treated with vitisin B for 24 h and then evaluated using an MTS assay. Bar graph (mean ± SEM) statistics were determined by the results of experiments ($n = 6$) using a one-way ANOVA with Tukey's *post hoc* test, ***$P < 0.001$; **$P < 0.01$ compared with the untreated group (0).

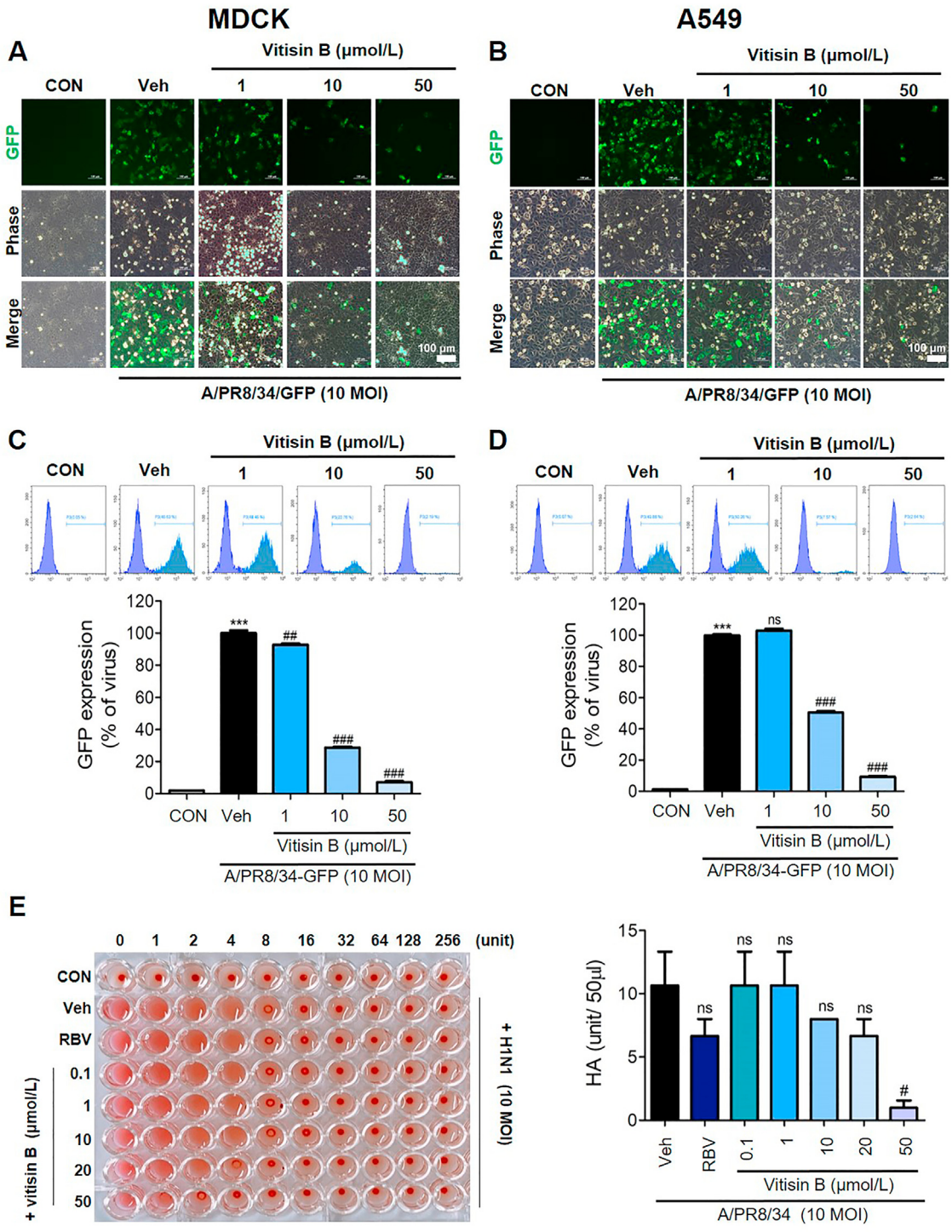

Figure 4 Antiviral effects of vitisin B on influenza A virus in MDCK and A549 cells. The cells were co-treated with various concentrations of vitisin B (1, 10, and 50 μmol/L) and influenza A viruses (A/PR/8/34/GFP and A/PR/8/34) and then the GFP levels were detected under a fluorescence microscope in (A) MDCK and (B) A549 cells. Scale bar = 100 μm. (C, D) Quantitative analysis was done by flow cytometry. (E) Viruses were titrated from the supernatant using a hemagglutinin assay. (F) Expression of M1, NS1, PA, and PB1 mRNA was measured by qRT-PCR. (G) Immunofluorescence analysis indicating the level of influenza A virus NA in A549 cells. Scale bar = 200 μm. Influenza A virus protein levels in cell lysates were analyzed by Western blot analysis and quantitated using Image J software in (H, I) MDCK and (J, K) A549 cells. Bar graph (mean ± SEM) analysis was determined by the results of experiments ($n = 4$) using a one-way ANOVA with Tukey's *post hoc* test, $^{***}P < 0.001$ compared with the untreated group (CON). $^{\#\#\#}P < 0.001$; $^{\#\#}P < 0.01$; $^{\#}P < 0.05$ compared with the virus-infected group (Veh). ns, not significance.

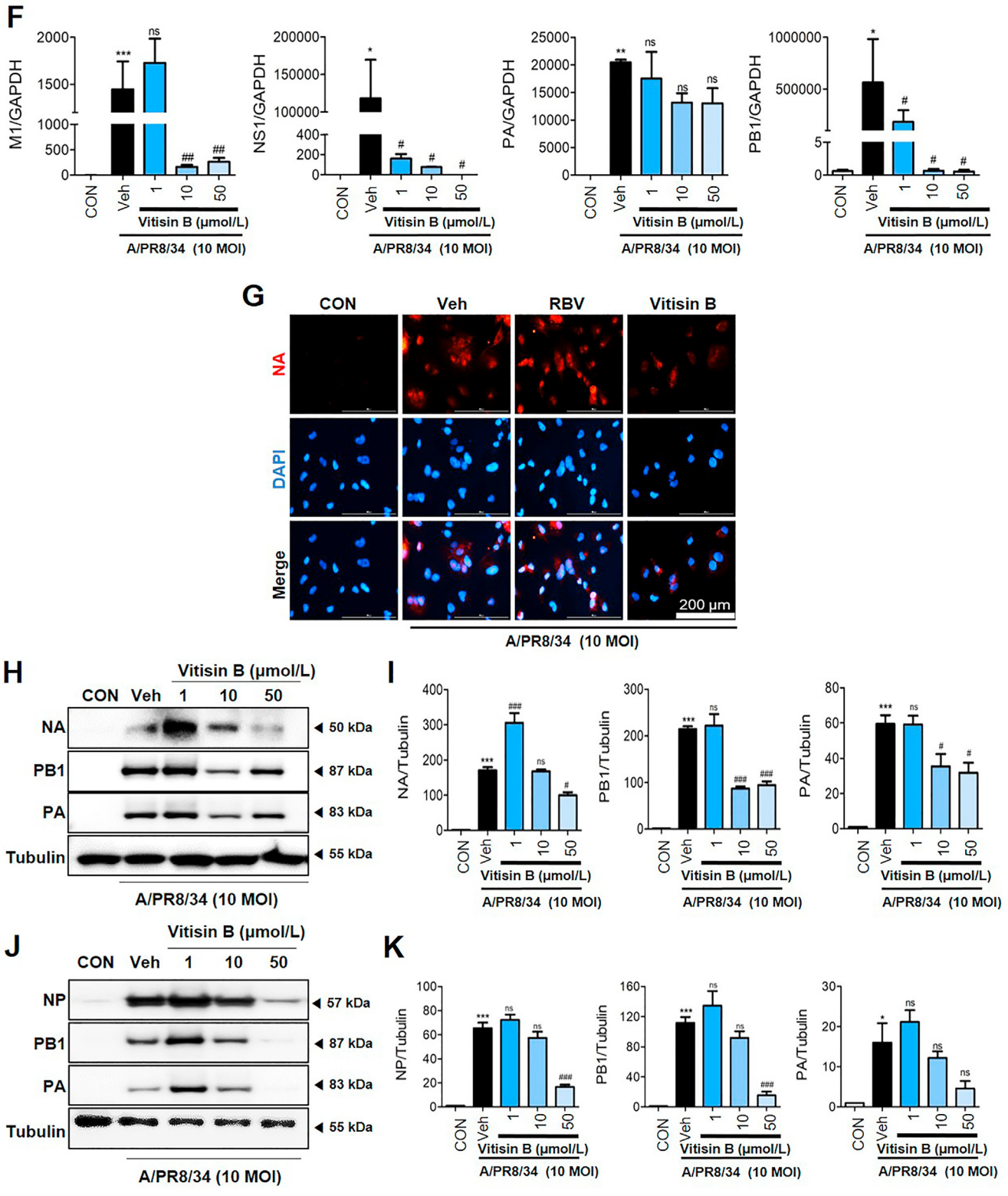

Figure 4 (*continued*).

infected host cells, using an *in silico* docking simulation[52–54]. The binding affinity of VB and the positive control, oseltamivir carboxylate, to H1N1 NA was predicted to be −6.6 and −9.9 kcal/mol, respectively (Fig. 5). Despite the stronger H1N1 NA inhibition of oseltamivir compared with VB (Fig. 2), the high binding affinity of VB from the docking simulations may have resulted from a marked interaction of the H1N1 NA–VB complex. Pharmacophore analysis revealed that VB strongly interacted with H1N1 NA by forming 30 interactions (7 conventional/1 carbon/1 pi–donor hydrogen bonds and 13 van der Waals/1

pi−cation/1 pi−anion/1 pi−sigma/5 pi−alkyl interactions) with H1N1 NA, whereas oseltamivir carboxylate formed 16 (4 conventional hydrogen bonds, and 11 van der Waals/1 alkyl interactions) with H1N1 NA[55]. The actual NA inhibitory activity was influenced by various factors, including protein−ligand interactions and the binding direction of ligands. Oseltamivir binding to H1N1 NA resulted in a rotation of E276 to form a salt bridge with R224, which created a hydrophobic pocket in the H1N1 NA. The hydrophobic oseltamivir pentyl ether group was parallel to E276 and interacted with the hydrophobic I222, enabling strong NA inhibition by oseltamivir[46−49]. However, VB did not interact with the critical residues R224 and E2762 during pharmacophore analysis, which may have contributed to the difference in NA inhibition between oseltamivir and VB.

3.5. *NF-κB inactivation contributes to the anti-IAV effect of VB*

NF-κB regulates various cellular processes, including the inflammatory response, cell survival, and apoptosis[50]. Furthermore, NF-κB is a major host signaling pathway implicated in influenza virus replication. In fact, a previous study demonstrated that infection with influenza viruses activates the NF-κB signaling pathway[56,57]. In the present study, we examined the effects of VB on NF-κB translocation to the nucleus. We also determined the phosphorylation status of p65, a functional subunit of NF-κB complex, in the cytoplasm and nucleus. As shown in Fig. 6A and B, VB inhibited NF-κB translocation to the nucleus and reduced p65/NF-κB protein expression in the nucleus, thus inhibiting influenza virus infection. The nuclear extracts of A549cells, incubated in the presence or absence of VB, were analyzed using DIG-labeled oligonucleotides corresponding to the NF-κB sites. NF-κB−DNA formation was prominent in nuclear extracts from influenza-infected A549 cells. However, NF-κB binding activity was remarkably suppressed in influenza-infected A549 cells when they were treated with VB (Fig. 6C). Previous studies have indicated that MAPKs, IκB proteins, and IκB kinase (IKK) are upstream regulators of NF-κB[58]. Therefore, we determined whether VB upregulates these signaling pathways by measuring total protein by Western blot analysis. Influenza virus infection dramatically increased the phosphorylation of IKK, JNK, and STAT1. However, VB decreased virus-induced phosphorylation of IKK, JNK, and STAT1 (Fig. 6D and E). Collectively, these data suggest that VB inhibited the translocation of NF-κB through decreased phosphorylation of the IKK pathway.

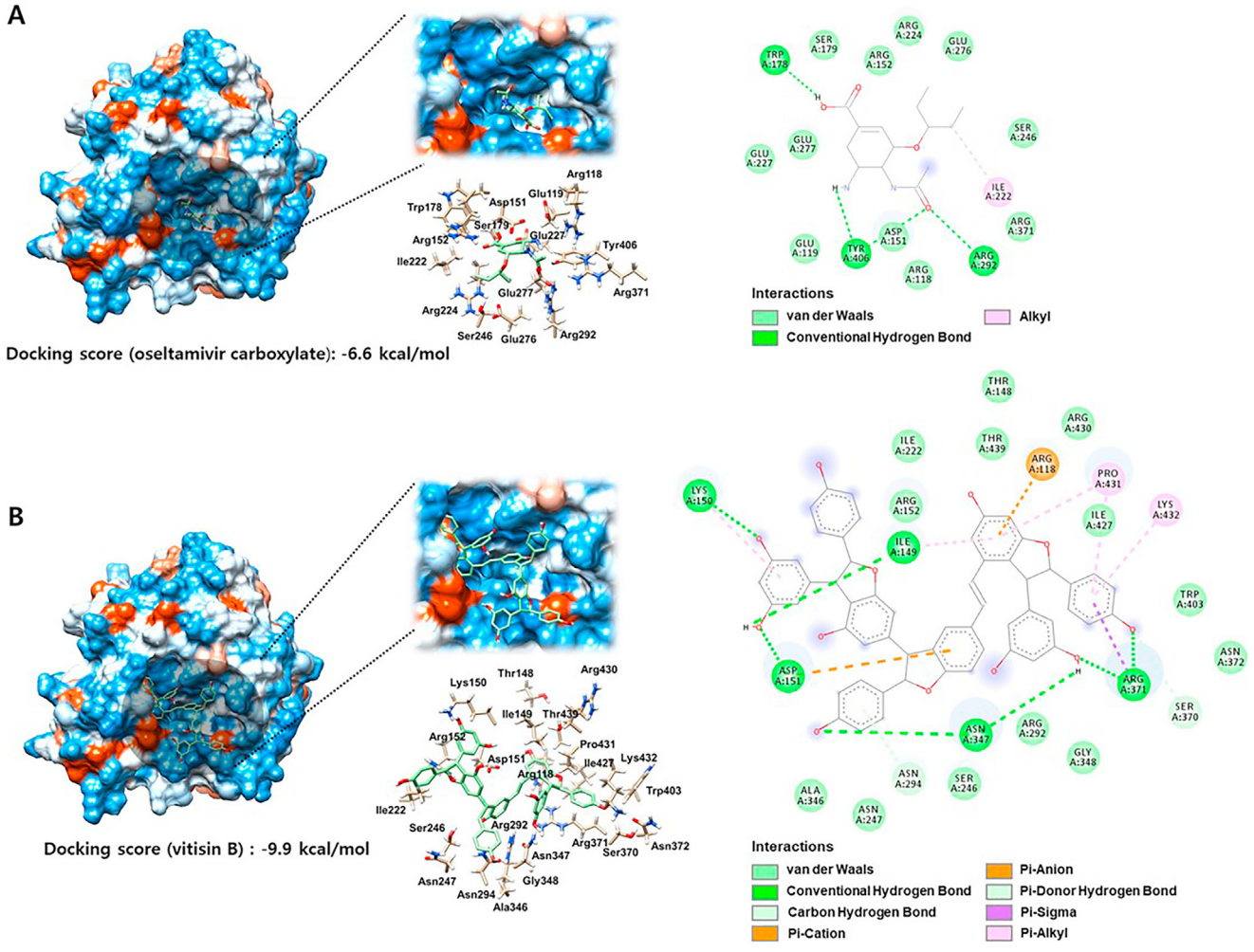

Figure 5 Docking simulation of vitisin B to the active site of the NA protein of influenza virus H1N1 (3TI6 A chain). Computational structure prediction for docking between (A) oseltamivir carboxylate (OTC) or (B) vitisin B and the NA protein. The binding interaction was further evaluated with LigPlot + v1.4.5.

3.6. VB inhibits virus-induced cellular ROS

IAV infection contributes to ROS production by stress in the endoplasmic reticulum and mitochondria. In particularly, excess ROS production causes an impaired redox balance, leading to apoptosis and inflammation in the host cells[28,59]. In addition, IAV-mediated ROS regulates signaling pathways, such as p38/JNK/MAPK and NF-κB[53]. To determine whether VB decreases cellular ROS levels in IAV-infected A549 cells, ROS levels were measured using DCF-DA, HE, and mitoSOX. As shown in Fig. 7A and D, H_2O_2 and O_2^- were measured using DCF-DA and HE, respectively. VB inhibited the levels of H_2O_2 and O_2^- in IAV-infected A549 cells in a dose-dependent manner (Fig. 7A and B). Furthermore, mitochondrial ROS (mtROS) levels were measured using mitoSOX. The results indicate that VB inhibited mtROS levels in IAV-infected A549 cells (Fig. 7C and D). Redox homeostasis is maintained by cellular enzymes, such as SOD, CAT, and GPx, which participate in antioxidant defense systems[25]. Western blot analysis was performed to confirm the expression levels of antioxidant enzymes, such as SOD and CAT. As shown in Fig. 7E and F, the expression of SOD and CAT decreased during viral infection, but the expression of both proteins increased following VB treatment. In addition, VB increased CAT and SOD activities (Fig. 7G). Altogether, these data demonstrate that IAV infection induced ROS production and reduces antioxidant enzyme activity; however, VB marginally suppressed cellular ROS and increases antioxidant enzymes in IAV-infected A549 cells.

3.7. VB improves Nrf2 expression on IAV-infected A549 cells

We confirmed in our results that VB increased antioxidant enzymes, such as SOD and CAT, which were reduced by viral infection. Therefore, it was investigated whether there was an effect following Nrf2 expression, which is an up-regulator of SOD and CAT and a key regulator of redox homeostasis. ROS accumulation induced Nrf2 translocation to the nucleus, leading to transcription for antioxidant enzymes, such as SOD, CAT, and GSH synthesis[34,35]. To determine whether VB increased Nrf2 translocation to the nucleus. As shown in Fig. 8A and B, VB increased Nrf2 nuclear translocation and phosphorylation, which was reduced by IAV infection. G6PD regulates oxidative stress

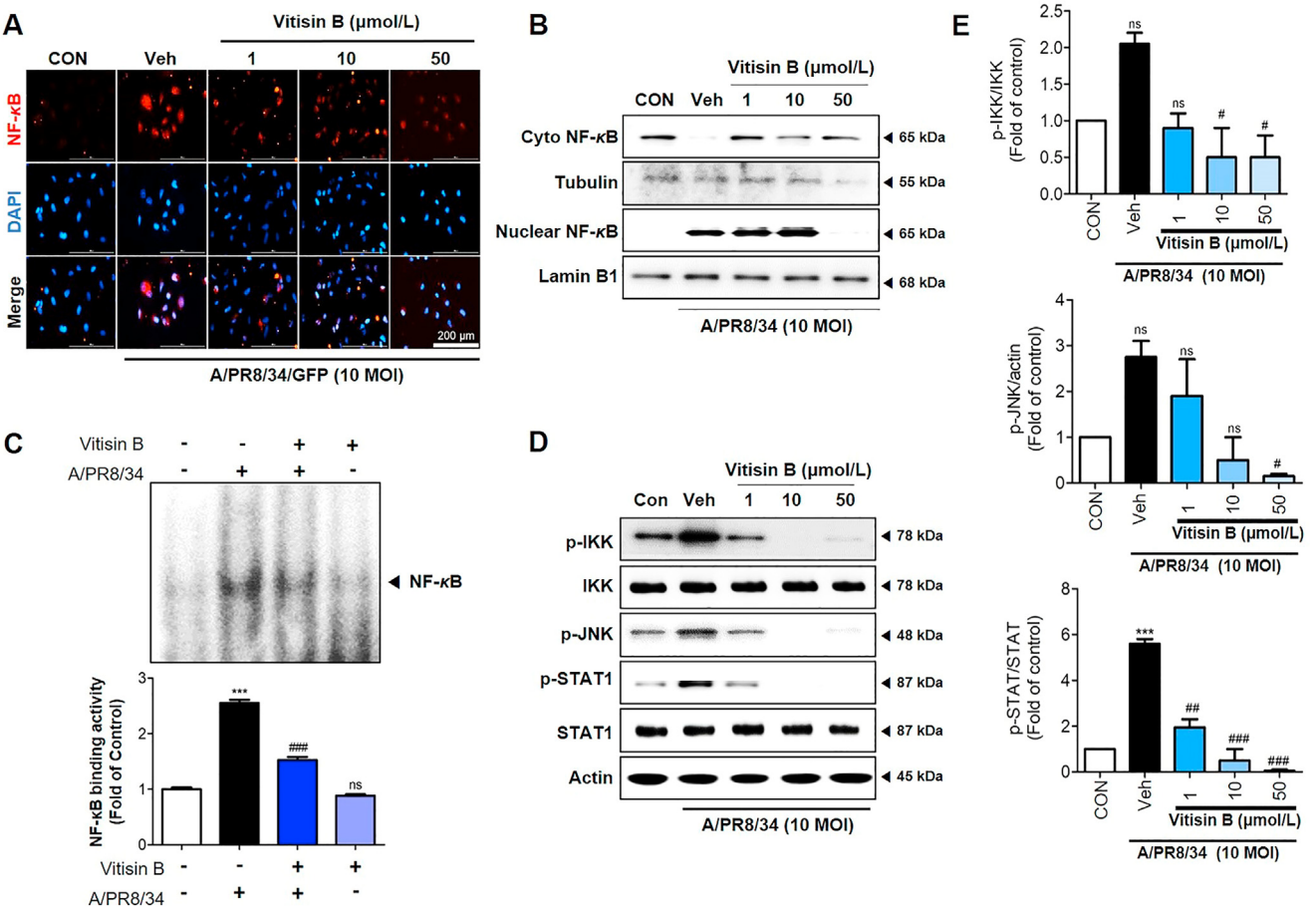

Figure 6 Vitisin B inhibits NF-κB translocation by influenza A virus infection in A549 cells. Cells were co-infected with influenza A virus and various concentrations of vitisin B for 24 h. (A) Cellular NF-κB was analyzed by immunofluorescence assay. Scale bar = 200 μm. (B) Evaluation of the levels of cytosolic and nuclear NF-κB in cell lysates. (C) VB suppresses the binding activity of NF-κB in influenza-infected A549 cells. DNA-binding activity of NF-κB in nuclear extracts was measured by EMSA. (D, E) Western blot analysis was performed using whole-cell lysates to assess the expression of total and phosphorylated IKK, JNK, and STAT1. Quantitative analysis was performed using Image J software. Bar graph (mean ± SEM) analysis was determined by the results of experiments ($n = 4$) using a one-way ANOVA with Tukey's *post hoc* test, $^{***}P < 0.001$ compared with the untreated group (CON). $^{###}P < 0.001$; $^{##}P < 0.01$; $^{#}P < 0.05$ compared with the virus-infected group (Veh). ns, not significance.

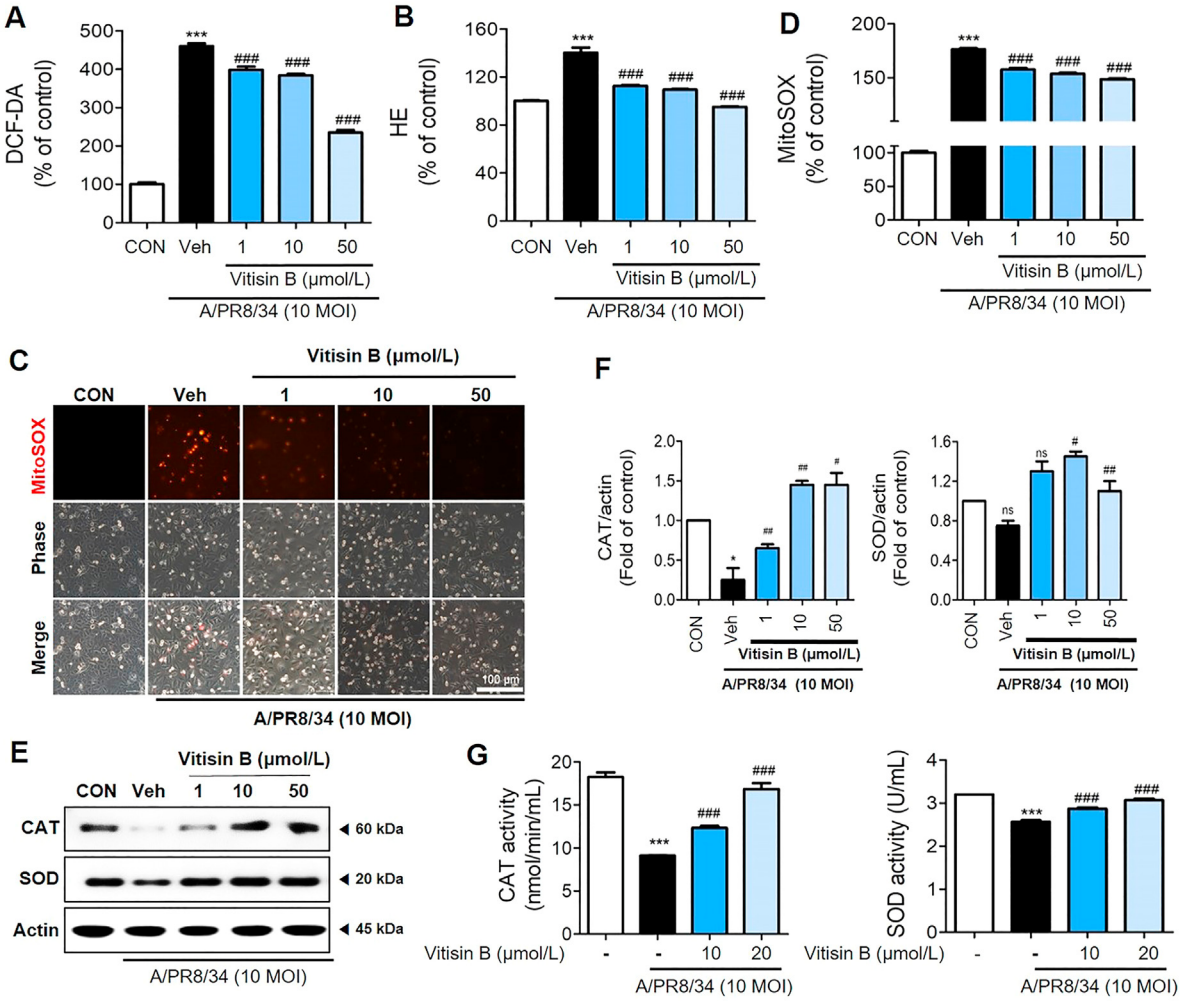

Figure 7 Vitisin B inhibits ROS production by influenza A virus infection in A549 cells. Cells were co-infected with vitisin B and influenza A virus and then ROS was detected using (A) DCF-DA, (B) HE, and (C, D) mitoSOX. The level of ROS was measured flow cytometry. Scale bar = 100 μm. (E, F) Antioxidant enzyme activity, such as CAT and SOD levels, in cell lysates were analyzed by Western blot analysis and quantitated using Image J software. (G) CAT and SOD activities were measured using an assay kit. Bar graph (mean ± SEM) analysis was determined by the results of experiments ($n = 4$) using a one-way ANOVA with Tukey's *post hoc* test, $^{***}P < 0.001$ compared with the untreated group (CON). $^{\#\#\#}P < 0.001$; $^{\#\#}P < 0.01$; $^{\#}P < 0.05$, compared with the virus-infected group (Veh). ns, not significance.

through involvement in reduced GSH regeneration from its oxidized form as GSSG, a reaction catalyzed by glutathione reductase[34]. Accordingly, we examined VB effect on G6PD expression. The data show that VB increased G6PD expression in reduced IAV-infected A549 cells (Fig. 8C). In addition, it was confirmed that VB increased the GSH/GSSH ratio reduced by IAV infection in A549 cells (Fig. 8D). Taken together, virus infection decreased by the Nrf2-mediated antioxidant response, such as G6PD downregulation; however, VB treatment increased the translocation of Nrf2 to the nucleus and G6PD expression. Thus, the data suggest that VB contributed to improving antioxidant response in IAV-infected A549 cells.

3.8. *VB inhibited IAV infection in BALB/c mice*

Next, we determined the antiviral effects of VB against IAV infection in mice. We measured survival and body weight following daily administration of VB in IAV-infected mice. The infected mice exhibited significant bodyweight loss by 5−7 dpi, which resulted in death within 9 dpi compared with the control mice. In contrast, VB-treated mice exhibited decreased mortality and increased survival rates compared with IAV-infected mice (Fig. 9A). Furthermore, an increase in body weight was observed in VB-treated mice compared with IAV-infected mice (Fig. 9B). Furthermore, immunofluorescent images indicate that the NA viral protein was decreased in the lungs of VB-treated mice compared with that of IAV-infected mice (Fig. 9C). We dissected the mouse lungs ($n = 3$) and combined them into one sample for RNA and protein isolated. We confirmed the expression level of the viral proteins by qRT-PCR and Western blot analysis. Both PCR and Western blot results indicate that VB markedly reduced the mRNA levels of *NS1*, *HA*, *M2*, and *PB1* in IAV-infected lung tissues (Fig. 9D−F). These data indicate that VB inhibited viral replication in IAV-infected mice.

3.9. *VB inhibited inflammation response in IAV-infected BALB/c mice*

The mouse lungs were sampled at 8 dpi and stained with hematoxylin and eosin (H&E) to identify histopathological changes

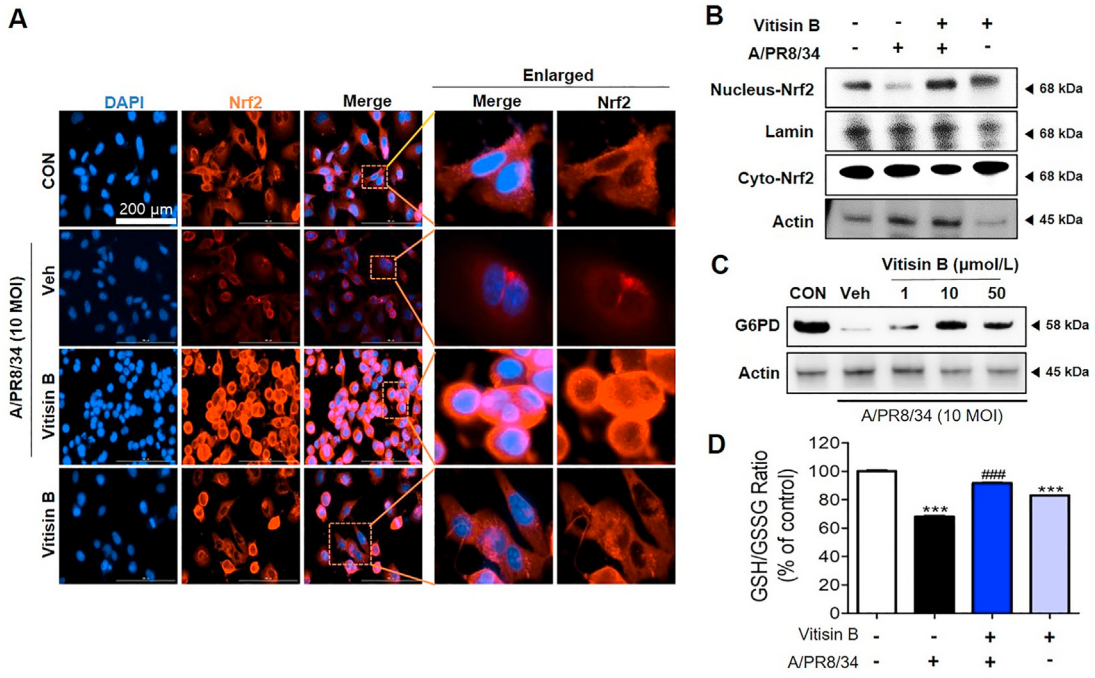

Figure 8 Effects of vitisin B on Nrf2-mediated antioxidant response in IAV-infected A549 cells. Cells were co-infected with influenza A virus and various concentrations of vitisin B for 24 h. (A) Cellular Nrf2 was analyzed by immunofluorescence assay. Scale bar = 200 μm. (B) Evaluation of the levels of cytosolic and nuclear Nrf2 in cell lysates. (C) Western blotting was performed using whole-cell lysates to assess G6PD expression. (D) Intracellular GSH/GSSG ratio measured after 24 h from infection by colorimetric assay as described in the section Methods and represented as percentage (%) respect to control cells. Bar graph (mean ± SEM) analysis was determined by the results of experiments ($n = 4$) using a one-way ANOVA with Tukey's *post hoc* test, $^{***}P < 0.001$ compared with the untreated group (CON). $^{\#\#\#}P < 0.001$ compared with the virus-infected group (Veh).

caused by viral infection. The histological sections show that the bronchial epithelial cells had significantly thickened alveolar walls and pulmonary congestion in IAV-infected mice compared with the control mice. These changes were ameliorated considerably by administering VB or OP (Fig. 10A). In addition, the results of blinded histological patterns after H&E staining revealed that IAV infection induced inflammation in the lungs. We evaluated inflammatory factors, such as TNF-α and IL-6, using mouse serum and RNA and protein isolated from the lungs. The results indicate that VB treatment decreased TNF-α and IL-6 levels in the serum and IAV-infected lung tissues (Fig. 10B−E). Taken together, these results confirm that the inflammatory response increased by viral infection was significantly ameliorated by VB.

4. Discussion

Long-term use of anti-influenza virus agents, such as oseltamivir, results in the emergence of drug-resistant mutated strains as well as side effects[60]. Therefore, the development of new drugs is needed as an anti-influenza strategy based on novel targets and reinforcement of the existing drug paradigm.

NA is a glycoprotein present on the surface of the influenza virus that is required for the release of progeny virions from infected host cells by cleaving sialic acid moieties on the cell surface that bind to viral hemagglutinin[61]. NAIs prevent the release of progeny virions by interacting with the highly conserved active site of NA. However, a recent study demonstrated that H274Y, E119G/D/A, H274Y, and mutations of NA decrease virus susceptibility to NAIs, such as oseltamivir, zanamivir, and peramivir, resulting in a need for new antiviral agents[9−19]. Nevertheless, NA remains an attractive target for the development of anti-influenza drugs. Novel and effective antiviral agents for preventing and treating viral infections, such as SARS-CoV-2 and influenza, may be present in natural products.

In the present study, we observed significant *in vitro* activity of VB isolated from *V. vinifera* stem bark against IAV infection through the inhibition of NA activity by direct binding to this viral protein. Upon examining the structure−activity relationship of VB and related constituents, we had some interesting discoveries. Ampelopsin A and ε-viniferin exhibited weak inhibitory effects; however, when ampelopsin A unit was incorporated along with the ε-viniferin unit (vitisin A and *cis*-vitisin A), the antiviral effects increased significantly. Furthermore, VB, which contains two units of ε-viniferin, exhibited the strongest inhibitory effect against NA. Therefore, the ε-viniferin unit conjunction appears to be a key functional element. These data will be useful in evaluating the structure−activity relationships of related constituents and developing new antiviral agents (Fig. 11).

VB improved cell viability and reduced infection of influenza viruses, including H1N1, H3N2, IBV in MDCK cells and oseltamivir-resistant A/PR8/34 in A549 cells. Also, VB reduced GFP-encoded IAV infection in MDCK and A549 cells. VB also suppressed mortality and retained body weight compared with viral infection alone and it reduced the inflammatory response. These results accentuated the potential of VB against IAV infection.

NAI (oseltamivir, zanamivir, and peramivir)-resistant influenza viruses have emerged because of mutations in E119, H274, R292, and N294 of NA. Therefore, research into the antiviral efficacy of

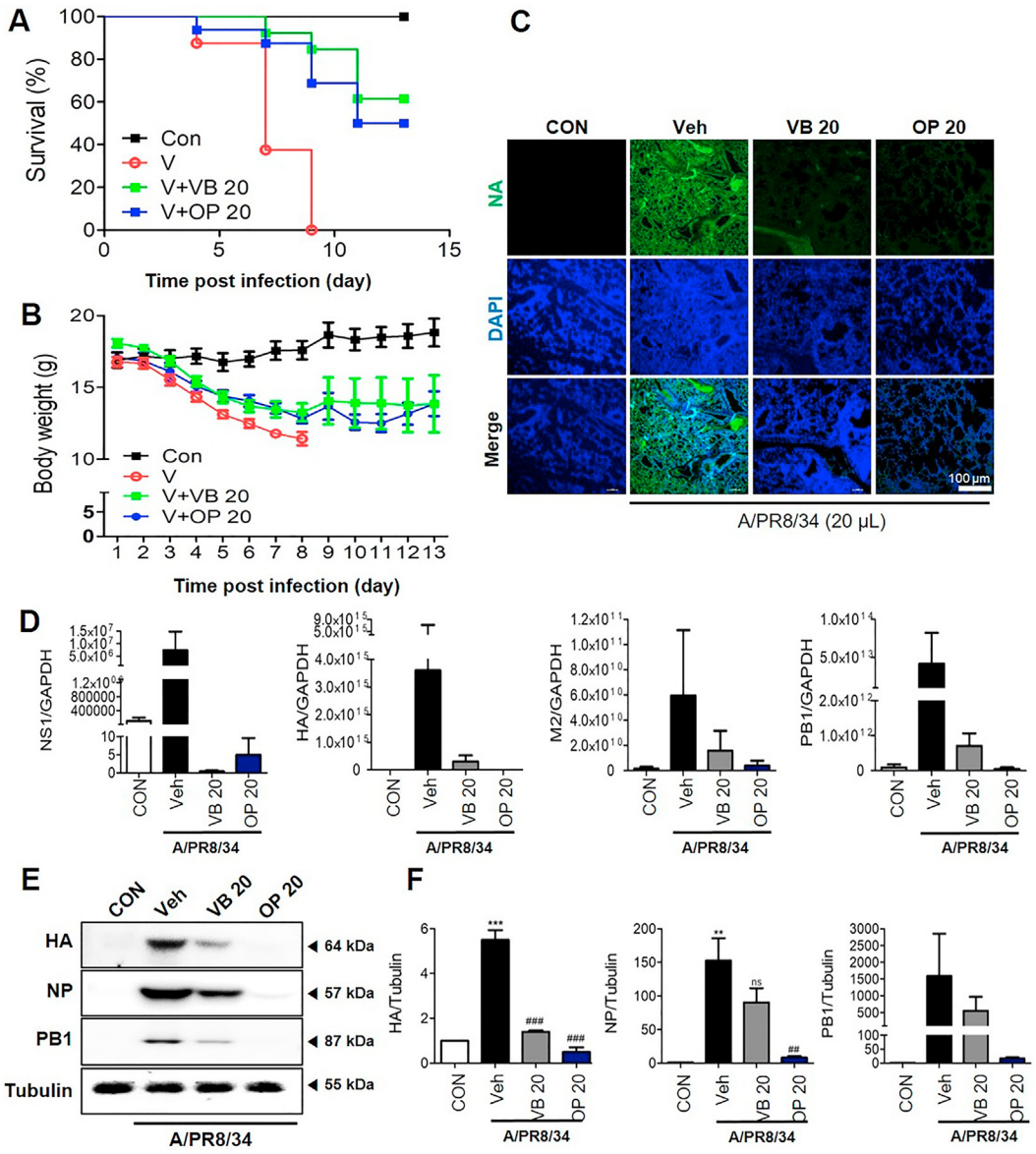

Figure 9 Effects of vitisin B on influenza A virus infection in BALB/c mice. Mouse nasal cavities were infected with influenza A virus after oral administration with 20 mg/kg vitisin B. (A) Percent survival and (B) body weight were monitored daily until 7 days post-infection. (C) Immunofluorescence analysis revealed the levels of influenza A virus NA in virus-infected mouse lung. Scale bar = 100 μm. (D) Expression of viral genes were measured using qRT-PCR in mouse lung lysates. (E, F) Influenza A virus protein levels in the cell lysates were analyzed by Western blot analysis and quantitated using Image J software. Bar graph (mean ± SEM) statistics were determined by the results of experiments ($n = 10$) using a one-way ANOVA with Tukey's *post hoc* test, $^{***}P < 0.001$ compared with the untreated group (CON). $^{\#\#\#}P < 0.001$; $^{\#\#}P < 0.01$, compared with the virus-infected group (Veh). ns, not significance.

natural products, including VB, against these resistant viruses is of significant interest. Here, OC was ineffective against OC-resistant viruses; however, VB was effective against them. The results could be proposed as an attractive treatment for viral strains resistant to conventional NA inhibitors.

To determine the antiviral mechanism of VB, we evaluated NF-κB and ROS levels during infection. NF-κB and ROS have important roles in viral replication and the inflammatory response in host cells. Studies have demonstrated that overexpression of the HA, NP, and M1 viral proteins may activate the NF-κB signaling pathway. Other studies have demonstrated that activation of NF-κB is required for viral replication and promotes the transcription of inflammatory genes, leading to a robust inflammatory response. Therefore, inactivating NF-κB is associated with antiviral effects. In this study, we demonstrate that VB interferes with NF-κB activation by inhibiting IKK and JNK phosphorylation, which contributes to the antiviral effects against IAV infection. Furthermore, influenza virus infection causes an imbalance of redox homeostasis by increasing ROS production and GSH depletion in host cells. G6PD restores NADPH dependent GSH level and is related to the Nrf2 pathway. In addition, decreased G6PD expression leads to increased viral replication and oxidative stress. Therefore, Nrf2-mediated G6PD pathway is an interesting target in virus-infection induced oxidative stress. Moreover, VB reduces ROS generation and increases Nrf2-mediated antioxidant gene expression as G6PD during IAV infection.

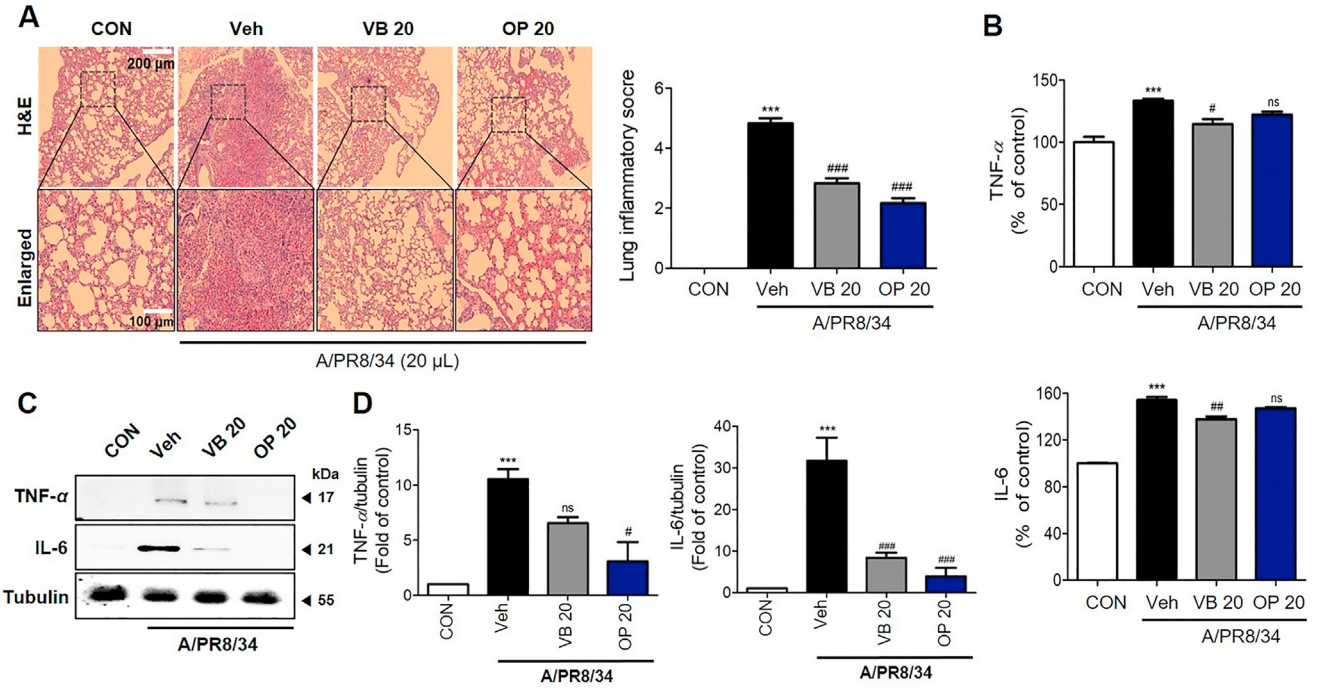

Figure 10 Effects of vitisin B on inflammation in influenza A virus-infected BALB/c mice. (A) A representative H&E image showing the histopathological damage in sectioned lung tissue of untreated mice and mice treated with vitisin B. (B) Serum TNF-α and IL-6 levels were measured using an ELISA kit. (C, D) TNF-α and IL-6 levels in the lung lysates were analyzed by Western blot analysis and quantitated using Image J software. Bar graph (mean ± SEM) statistics were determined by the results of experiments ($n = 3$) using a one-way ANOVA with Tukey's *post hoc* test, $^{***}P < 0.001$ compared with the untreated group (CON). $^{\#\#\#}P < 0.001$; $^{\#\#}P < 0.01$; $^{\#}P < 0.05$, compared with the virus-infected group (Veh). ns, not significance.

Studies have established that antioxidants, such as glutathione and *N*-acetyl-L-cysteine (NAC), increase the host defense against influenza infection[62,63].

However, NAC does not directly exhibit antiviral effects on influenza infection *in vitro* and reduces viral mortality in *in vivo* experiments. NAC increases survival by reducing the inflammatory response of lung tissues and enhancing the host defense mechanism and oxidative stress control[64]. VB alleviated the inflammatory response based on mouse lung histology, indicating that ROS downregulation has no direct effect on antiviral activity,

Compound	NA inhibition (10 μmol/L)
Ampelopsin A	> 80%
ε-Viniferin	> 80%
Vitisin A	50 – 65%
cis-Vitisin A	50 – 65%
Vitisin B	**< 40%**

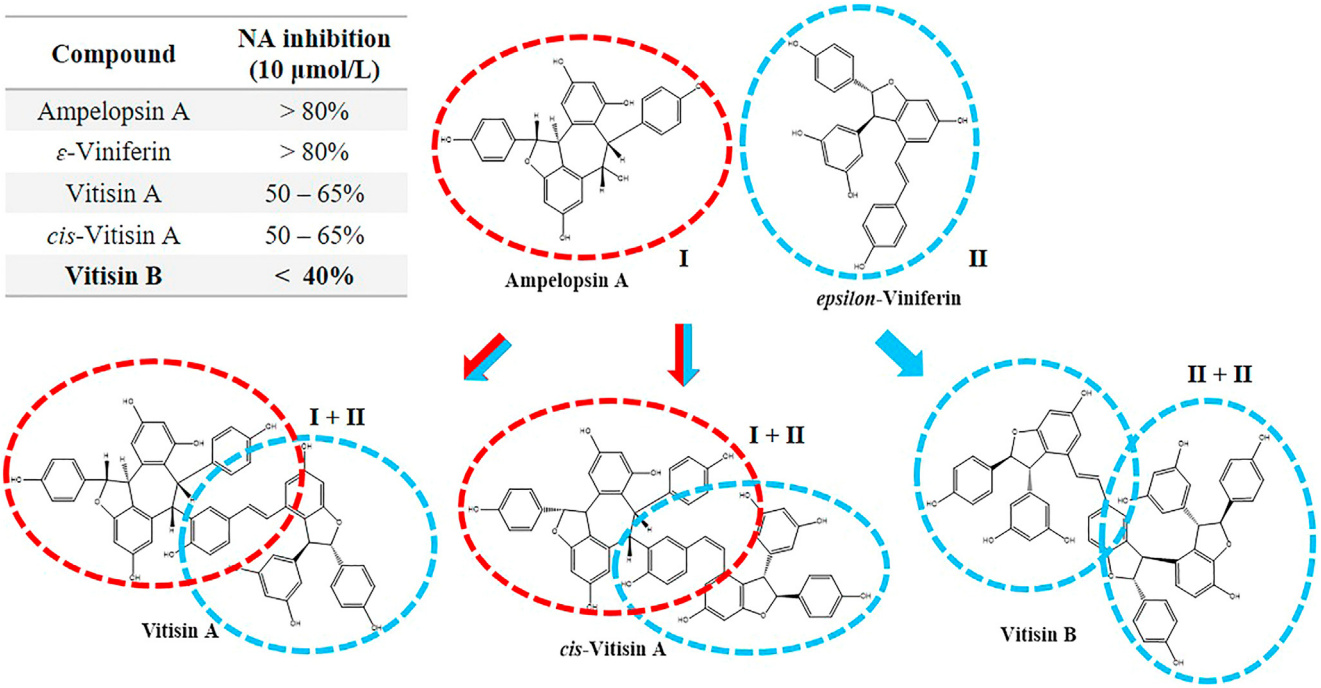

Figure 11 Structure−activity relationship between vitisin B and related compounds.

but may inhibit viral replication and the inflammatory response through a ROS-mediated NF-κB dual mechanism. However, based on previous results, VB has a direct effect on NA and significantly inhibits its activity. The combined administration of the NAI, oseltamivir, and NAC to IAV-infected mice showed a synergistic effect compared with either treatment alone[65]. Based on these results, we suggest that VB exhibits antiviral effects by multi-targeting through NA and antioxidative response. In addition, a recent study indicated that SARS-CoV-2, a type of RNA virus that has recently emerged as a global issue, increases ROS production by inducing oxidative stress and cytokine secretion, inflammation, and cell death through NF-κB activation in host cells[66−68]. Therefore, it is anticipated that VB will be effective against the SARS-CoV-2 virus, but this should be confirmed in future studies. Therefore, naturally-derived VB has potential as a novel therapeutic agent for infectious diseases.

5. Conclusions

Our study indicates that VB is effective against IAV infection. The antiviral effect of VB was demonstrated by multi-targeting through the inhibition of the NA viral protein and suppression of ROS production. In addition, VB ameliorated the inflammatory response through NF-κB downregulation, decreased ROS generation, and increased expression of Nrf2-mediated antioxidant gene as G6PD during IAV infection. Therefore, our study suggests that VB is a useful drug for treating IAV infection and related diseases.

Acknowledgments

This work was supported by the National Research Foundation of Korea (NRF) grant funded 2021R1A2C2094436 and 2020R1C1C1006749 and the Korea Institute of Oriental Medicine grant number KSN2022230 provided by the Ministry of Science and ICT, Korea.

Author contributions

Eun-Bin Kwon, Wei Li, and Jang-Gi Choi conceived and designed the manuscript. Eun-Bin Kwon, Wei Li, Young-Soo Kim, Buyun Kim, Hwan-Suck Chung, hyun-Jeong Ko and Jae-Hyoung Song, Young Ho Kim, Chun Whan Choi, and Jang-Gi Choi contributed to methodology, validation, and writing of the manuscript. Eun-Bin Kwon, Wei Li, Young Ho Kim, Chun Whan Choi, and Jang-Gi Choi critically reviewed the manuscript. Funding acquisition: Wei Li, Hwan-Suck Chung, and Jang-Gi Choi. All authors have read and agreed to the published version of the manuscript.

Conflicts of interest

The authors declare no conflicts of interest.

Appendix A. Supporting information

Supporting data to this article can be found online at https://doi.org/10.1016/j.apsb.2022.07.001.

References

1. Hussain M, Galvin HD, Haw TY, Nutsford AN, Husain M. Drug resistance in influenza A virus: the epidemiology and management. *Infect Drug Resist* 2017;**10**:121.
2. Bouvier NM, Palese P. The biology of influenza viruses. *Vaccine* 2008;**26**:D49−53.
3. Chen J, Deng YM. Influenza virus antigenic variation, host antibody production and new approach to control epidemics. *Virol J* 2009;**6**:30.
4. Naesens L, Stevaert A, Vanderlinden E. Antiviral therapies on the horizon for influenza. *Curr Opin Pharmacol* 2016;**30**:106−15.
5. Vanderlinden E, Naesens L. Emerging antiviral strategies to interfere with influenza virus entry. *Med Res Rev* 2014;**34**:301−39.
6. Okomo-Adhiambo M, Sheu TG, Gubareva LV. Assays for monitoring susceptibility of influenza viruses to neuraminidase inhibitors. *Influenza Other Respir Viruses* 2013;**7**:44−9.
7. Ilyushina NA, Komatsu TE, Ince WL, Donaldson EF, Lee N, O'Rear JJ, et al. Influenza A virus hemagglutinin mutations associated with use of neuraminidase inhibitors correlate with decreased inhibition by anti-influenza antibodies. *Virol J* 2019;**16**:149.
8. Villalón-Letelier F, Brooks AG, Saunders PM, Londrigan SL, Reading PC. Host cell restriction factors that limit influenza A infection. *Viruses* 2017;**9**:376.
9. Gubareva LV. Molecular mechanisms of influenza virus resistance to neuraminidase inhibitors. *Virus Res* 2004;**103**:199−203.
10. Hurt AC, Holien JK, Parker MW, Barr IG. Oseltamivir resistance and the H274Y neuraminidase mutation in seasonal, pandemic and highly pathogenic influenza viruses. *Drugs* 2009;**69**:2523−31.
11. Hamelin MÈ, Baz M, Abed Y, Couture C, Joubert P, Beaulieu E, et al. Oseltamivir-resistant pandemic A/H1N1 virus is as virulent as its wild-type counterpart in mice and ferrets. *PLoS Pathog* 2010;**6**:e1001015.
12. Bai Y, Jones JC, Wong SS, Zanin M. Antivirals targeting the surface glycoproteins of influenza virus: mechanisms of action and resistance. *Viruses* 2021;**13**:624.
13. Baek YH, Song MS, Lee EY, Kim YI, Kim EH, Park SJ, et al. Profiling and characterization of influenza virus N1 strains potentially resistant to multiple neuraminidase inhibitors. *J Virol* 2015;**89**:287−99.
14. Samson M, Pizzorno A, Abed Y, Boivin G. Influenza virus resistance to neuraminidase inhibitors. *Antivir Res* 2013;**98**:174−85.
15. Nguyen HT, Fry AM, Gubareva LV. Neuraminidase inhibitor resistance in influenza viruses and laboratory testing methods. *Antivir Ther* 2012;**17**:159.
16. Choi WS, Jeong JH, Kwon JJ, Ahn SJ, Lloren KKS, Kwon HI, et al. Screening for neuraminidase inhibitor resistance markers among avian influenza viruses of the N4, N5, N6, and N8 neuraminidase subtypes. *J Virol* 2018;**92**:e01580-17.
17. Memoli MJ, Hrabal RJ, Hassantoufighi A, Eichelberger MC, Taubenberger JK. Rapid selection of oseltamivirand peramivir-resistant pandemic H1N1 virus during therapy in 2 immunocompromised hosts. *Clin Infect Dis* 2010;**50**:1252−5.
18. Pizzorno A, Bouhy X, Abed Y, Boivin G. Generation and characterization of recombinant pandemic influenza A (H1N1) viruses resistant to neuraminidase inhibitors. *J Infect Dis* 2011;**203**:25−31.
19. Thorlund K, Awad T, Boivin G, Thabane L. Systematic review of influenza resistance to the neuraminidase inhibitors. *BMC Infect Dis* 2011;**11**:134.
20. Nordberg J, Arnér ES. Reactive oxygen species, antioxidants, and the mammalian thioredoxin system. *Free Radic Biol Med* 2011;**31**:1287−312.
21. Chen KK, Minakuchi M, Wuputra K, Ku CC, Pan JB, Kuo KK, et al. Redox control in the pathophysiology of influenza virus infection. *BMC Microbial* 2020;**20**:1−22.
22. Lazrak A, Iles KE, Liu G, Noah DL, Noah JW, Matalon S. Influenza virus M2 protein inhibits epithelial sodium channels by increasing reactive oxygen species. *FASEB J* 2009;**23**:3829−42.
23. Wang R, Zhu Y, Lin X, Ren C, Zhao J, Wang F, et al. Influenza M2 protein regulates MAVS-mediated signaling pathway through

interacting with MAVS and increasing ROS production. *Autophagy* 2019;**15**:1163−81.
24. Sgarbanti R, Nencioni L, Amatore D, Coluccio P, Fraternale A, Sale P, et al. Redox regulation of the influenza hemagglutinin maturation process: a new cell-mediated strategy for anti-influenza therapy. *Antioxidants Redox Signal* 2011;**15**:593−606.
25. Liu M, Chen F, Liu T, Chen F, Liu S, Yang J. The role of oxidative stress in influenza virus infection. *Microb Infect* 2017;**19**:580−6.
26. McCarty MF, Barroso-Aranda J, Contreras F. Practical strategies for targeting NF-κB and NADPH oxidase may improve survival during lethal influenza epidemics. *Med Hypotheses* 2010;**74**:18−20.
27. Keshavarz M, Solaymani-Mohammadi F, Namdari H, Arjeini Y, Mousavi MJ, Rezaei F. Metabolic host response and therapeutic approaches to influenza infection. *Cell Mol Biol Lett* 2020;**25**:19.
28. Khomich OA, Kochetkov SN, Bartosch B, Ivanov AV. Redox biology of respiratory viral infections. *Viruses* 2018;**10**:392.
29. Ludwig S, Planz O. Influenza viruses and the NF-κB signaling pathway—towards a novel concept of antiviral therapy. *Biol Chem* 2008;**389**:1307−12.
30. Kabe Y, Ando K, Hirao S, Yoshida M, Handa H. Redox regulation of NF-κB activation: distinct redox regulation between the cytoplasm and the nucleus. *Antioxidants Redox Signal* 2005;**7**:395−403.
31. Gu Y, Hsu ACY, Pang Z, Pan H, Zuo X, Wang G, et al. Role of the innate cytokine storm induced by the influenza A virus. *Viral Immunol* 2019;**32**:244−51.
32. Khalili N, Karimi A, Moradi MT, Shirzad H. *In vitro* immunomodulatory activity of celastrol against influenza A virus infection. *Immunopharmacol Immunotoxicol* 2018;**40**:250−5.
33. Wei H, Wang S, Chen Q, Chen Y, Chi X, Zhang L, et al. Suppression of interferon lambda signaling by SOCS-1 results in their excessive production during influenza virus infection. *PLoS Pathog* 2014;**10**:e1003845.
34. Kido H, Okumura Y, Takahashi E, Pan HY, Wang S, Yao D, et al. Role of host cellular proteases in the pathogenesis of influenza and influenza-induced multiple organ failure. *Biochim Biophys Acta* 2012;**1824**:186−94.
35. De Angelis M, Amatore D, Checconi P, Zevini A, Fraternale A, Magnani M, et al. Influenza Virus Down-Modulates G6PD expression and activity to induce oxidative stress and promote its replication. *Front Cell Infect Microbiol* 2022;**6**:1372.
36. Sander WJ, Fourie C, Sabiu S, O'Neill FH, Pohl CH, O'Neill HG. Reactive oxygen species as potential antiviral targets. *Rev Med Virol* 2022;**32**:e2240.
37. Vlahos R, Stambas J, Selemidis S. Suppressing production of reactive oxygen species (ROS) for influenza A virus therapy. *Trends Pharmacol Sci* 2012;**33**:3−8.
38. Nencioni L, Sgarbanti R, Amatore D, Checconi P, Celestino I, Limongi D, et al. Intracellular redox signaling as therapeutic target for novel antiviral strategy. *Curr Pharmaceut Des* 2011;**17**:3898−904.
39. Lin LT, Hsu WC, Lin CC. Antiviral natural products and herbal medicines. *J Tradit Complement Med* 2014;**4**:24−35.
40. Verma S, Twilley D, Esmear T, Oosthuizen CB, Reid AM, Nel M, et al. Anti-SARS-CoV natural products with the potential to inhibit SARS-CoV-2 (COVID-19). *Front Pharmacol* 2020;**11**:1514.
41. Elfiky AA. Natural products may interfere with SARS-CoV-2 attachment to the host cell. *J Biomol Struct Dyn* 2021;**39**:3194−203.
42. Zhang ZJ, Morris-Natschke SL, Cheng YY, Lee KH, Li RT. Development of anti-influenza agents from natural products. *Med Res Rev* 2020;**40**:2290−338.
43. Grienke U, Schmidtke M, von Grafenstein S, Kirchmair J, Liedl KR, Rollinger JM. Influenza neuraminidase: a druggable target for natural products. *Nat Prod Rep* 2012;**29**:11−36.
44. Choi JG, Kim YS, Kim JH, Chung HS. Antiviral activity of ethanol extract of Geranii Herba and its components against influenza viruses *via* neuraminidase inhibition. *Sci Rep* 2019;**9**:12132.
45. Kwon EB, Yang HJ, Choi JG, Li W. Protective effect of flavonoids from *Ohwia caudata* against influenza a virus infection. *Molecules* 2020;**25**:4387.
46. Kim YS, Li W, Kim JH, Chung HS, Choi JG. Anti-influenza activity of an ethyl acetate fraction of a *Rhus verniciflua* ethanol extract by neuraminidase inhibition. *Oxid Med Cell Longev* 2020:8824934.
47. Choi JG, Lee H, Kim YS, Hwang YH, Oh YC, Lee B, et al. *Aloe vera* and its components inhibit influenza A virus-induced autophagy and replication. *Am J Chin Med* 2019;**47**:1307−24.
48. Insanu M, Karimah H, Pramastya H, Fidrianny I. Phytochemical compounds and pharmacological activities of *Vitis vinifera* L. *Appl Chem* 2021;**11**:13829−49.
49. Zannella C, Giugliano R, Chianese A, Buonocore C, Vitale GA, Sanna G, et al. Antiviral activity of *Vitis vinifera* leaf extract against SARS-CoV-2 and HSV-1. *Viruses* 2021;**13**:1263.
50. Séron K, Sahuc ME, Rouillé Y. Natural products and hepatitis C virus. *Nat Antimicrob Agents* 2018;**19**:289−327.
51. Hong EH, Song JH, Kim SR, Cho J, Jeong B, Yang H, et al. Morin hydrate inhibits influenza virus entry into host cells and has anti-inflammatory effect in influenza-infected mice. *Immune Network* 2020;**20**:e32.
52. Kim CU, Lew W, Williams MA, Liu H, Zhang L, Swaminathan S, et al. Influenza neuraminidase inhibitors possessing a novel hydrophobic interaction in the enzyme active site: design, synthesis, and structural analysis of carbocyclic sialic acid analogues with potent anti-influenza activity. *J Am Chem Soc* 1997;**119**:681−90.
53. Varghese JN, Smith PW, Sollis SL, Blick TJ, Sahasrabudhe A, McKimm-Breschkin JL, et al. Drug design against a shifting target: a structural basis for resistance to inhibitors in a variant of influenza virus neuraminidase. *Structure* 1998;**6**:735−46.
54. Taylor NR, Cleasby A, Singh O, Skarzynski T, Wonacott AJ, Smith PW, et al. Dihydropyrancarboxamides related to zanamivir: a new series of inhibitors of influenza virus sialidases. 2. Crystallographic and molecular modeling study of complexes of 4-amino-4*H*-pyran-6-carboxamides and sialidase from influenza virus types A and B. *J Med Chem* 1998;**41**:798−807.
55. Smith PW, Sollis SL, Howes PD, Cherry PC, Cobley KN, Taylor H, et al. Novel inhibitors of influenza sialidases related to GG167 structure−activity, crystallographic and molecular dynamics studies with 4*H*-pyran-2-carboxylic acid 6-carboxamides. *Bioorg Med Chem Lett* 1996;**6**:2931−6.
56. Gasparini C, Feldmann M. NF-κB as a target for modulating inflammatory responses. *Curr Pharmaceut Des* 2012;**18**:5735−45.
57. Kumar N, Xin ZT, Liang Y, Ly H, Liang Y. NF-κB signaling differentially regulates influenza virus RNA synthesis. *J Virol* 2008;**82**:9880−9.
58. Gaur P, Munjal A, Lal SK. Influenza virus and cell signaling pathways. *Med Sci Monit* 2011;**17**:RA148−54.
59. Panda S, Behera S, Alam MF, Syed GH. Endoplasmic reticulum & mitochondrial calcium homeostasis: the interplay with viruses. *Mitochondrion* 2021;**58**:227−42.
60. Loregian A, Mercorelli B, Nannetti G, Compagnin C, Palù G. Antiviral strategies against influenza virus: towards new therapeutic approaches. *Cell Mol Life Sci* 2014;**71**:3659−83.
61. Wagner R, Matrosovich M, Klenk HD. Functional balance between haemagglutinin and neuraminidase in influenza virus infections. *Rev Med Virol* 2002;**12**:159−66.
62. Uchide N, Toyoda H. Antioxidant therapy as a potential approach to severe influenza-associated complications. *Molecules* 2011;**16**:2032−52.
63. Geiler J, Michaelis M, Naczk P, Leutz A, Langer K, Doerr HW, et al. *N*-Acetyl-L-cysteine (NAC) inhibits virus replication and expression of pro-inflammatory molecules in A549 cells infected with highly pathogenic H5N1 influenza A virus. *Biochem Pharmacol* 2010;**79**:413−20.

64. Zhang RH, Li CH, Wang CL, Xu MJ, Xu T, Wei D, et al. *N*-Acetyl-L-cystine (NAC) protects against H9N2 swine influenza virus-induced acute lung injury. *Int Immunopharm* 2014;**22**:1−8.
65. Hui DS, Lee N. Adjunctive therapies and immunomodulating agents for severe influenza. *Influenza Other Respir Viruses* 2013;**7**:52−9.
66. Lippi A, Domingues R, Setz C, Outeiro TF, Krisko A. SARS-CoV-2: at the crossroad between aging and neurodegeneration. *Mov Disord* 2020;**35**:716−20.
67. Delgado-Roche L, Mesta F. Oxidative stress as key player in severe acute respiratory syndrome coronavirus (SARS-CoV) infection. *Arch Med Res* 2020;**51**:384−7.
68. Nasi A, McArdle S, Gaudernack G, Westman G, Melief C, Rockberg J, et al. Reactive oxygen species as an initiator of toxic innate immune responses in retort to SARS-CoV-2 in an ageing population, consider *N*-acetylcysteine as early therapeutic intervention. *Toxicol Rep* 2020;**7**:768−71.